Turkish Journal of Earth Sciences

Volume 33 | Number 3 Article 6

3-19-2024

Örenli metamorphics (Biga Peninsula, NW Anatolia): evidence for Triassic active continental margin of Paleo-Tethys Ocean

İSMAİL ONUR TUNÇ

TÜBİTAK

Turkish Journal of Earth Sciences

http://journals.tubitak.gov.tr/earth/

Research Article

Turkish J Earth Sci
(2024) 33: 326-340
© TÜBİTAK
doi:10.55730/1300-0985.1914

Örenli metamorphics (Biga Peninsula, NW Anatolia): evidence for Triassic active continental margin of Paleo-Tethys Ocean

İsmail Onur TUNÇ*
Department of Architecture and Urban Planning, Ezine Vocational School,
Çanakkale Onsekiz Mart University, Çanakkale, Turkiye

Received: 12.06.2023 • **Accepted/Published Online:** 17.12.2023 • **Final Version:** 19.03.2024

Abstract: The pre-Liassic basement of the Biga Peninsula, located in the westernmost part of the Sakarya Zone, consists of metamorphic assemblages that were considered to represent different continental basements in the north and south, and the suture (ophiolitic/mélange) zone(s) between them. The Çetmi mélange, defined as between these continental fragments (the Kazdağ Massif in the south and the Çamlıca Massif in the north) was evaluated as a subduction accretionary mélange of the Intra-Pontide Ocean and it was assumed that a suture passed through this part of the peninsula. This study was carried out on the most widely distributed outcrops of the Çetmi mélange(?) on the northwest flank of the Kazdağ Massif.

These units, which are named the Örenli metamorphics, are represented by a succession of low-grade metamorphic volcanic-volcaniclastic rocks and alternating metasedimentary rocks and recrystallized limestones. The tectonostratigraphically lowermost levels of the Örenli metamorphics are a blocky-chaotic assemblage, whereas the uppermost levels are a regular metavolcanic-metapelite succession, which passes upward into the Late Triassic recrystallized limestones, and is cut by very low-grade metamorphic diabase dykes of 165.81 ± 1.55 Ma age. Furthermore, metavolcanic rocks of this succession show a calc-alkaline association of Basalt-Andesite-Dacite-Rhyolite (BADR) pattern in the chemical classification diagram, which is the signature volcanic rock suite of convergent margins. In addition, all the metavolcanic rock samples show a significant enrichment in terms of incompatible elements and LIL elements and negative Nb and Ti anomalies on the MORB normalized multielement spider diagram, which indicates that these rocks characterize high-K calc-alkaline volcanism at the active continental margins.

Field relationships, zircon U-Pb geochronology, and geochemical data support that these units, outcropping in the study area, represent a Triassic active continental margin, most probably a fore-arc setting, related to the Paleo-Tethyan subduction, but not the subduction mélange of the Intra-Pontide Ocean.

Key words: Sakarya zone, Biga peninsula, Northwest Anatolia, Paleo-Tethyan active continental margin, Örenli metamorphics

1. Introduction

The Sakarya Zone has a pre-Liassic composite metamorphic basement (Okay et al., 1996; Göncüoğlu et al., 2000), represented by two main metamorphic assemblages: the Uludağ Group and the Yenişehir Group (Yılmaz et al., 1997). The Uludağ Group consists mainly of high-grade metamorphic schists, gneiss, amphibolites, and migmatites and is cut by Carboniferous granites (Yılmaz, 1977). The Yenişehir Group, on the other hand, is represented by a metaophiolite and metavolcanic-metasedimentary assemblage that has undergone glaucophane greenschist facies metamorphism (Yılmaz, 1977; Genç, 1993). The Yenişehir Group is overlain unconformably by shallow marine arkosic sandstones (Cambazkaya Formation; Saner, 1977) and limestones (Derbent limestone; Eroskay, 1965). A third assemblage representing the pre-Liassic basement of the Sakarya Zone is the Karakaya Formation (Bingöl et al., 1973) or Karakaya Complex (Şengör et al., 1984), represented by a Triassic sedimentary-volcanic assemblage. However, since the outcrops of the Karakaya Complex in the Sakarya Zone were sliced and mixed with the Uludağ and Yenişehir Group metamorphic rocks due to the Mesozoic and post-Mesozoic tectonics, there has been extensive debate on the stratigraphy, age, and tectonic setting of the unit (Yiğitbaş et al., 2018; Okay and Göncüoğlu, 2004 and references therein). The areas where the Triassic anchymetamorphic Karakaya Complex rocks were sliced with the metamorphic basement rocks of the Sakarya Zone (*i.e.* Uludağ and Yenişehir groups; Yılmaz et al., 1997) were defined as "Lower Karakaya Complex", and the parts less affected by tectonics were defined as "Upper Karakaya Complex" (Okay and Göncüoğlu, 2004).

* Correspondence: onurtunc@comu.edu.tr

In the Biga Peninsula, these metamorphic basement rocks of the Sakarya Zone are represented by the Kazdag Unit and the Kalabak Unit correlated with the Uludağ Group and the Yenişehir Group of Yılmaz et al. (1997), respectively (Figures 1A and 1B). It has been stated in previous studies (Okay et al., 1990; Okay and Satır, 2000; Beccaletto, 2004; Beccaletto et al., 2005; Duru et al., 2012) that there is a suture between the Çamlıca and Karabiga massifs in the north and the Kazdağ Massif in the south. The idea of the existence of this suture is based on a) the presence of the unit (Çetmi mélange), described as an ophiolitic mélange, and b) the interpretation that the metamorphic assemblages outcropping to the north and south represent two completely different continental basements. Field and analytical data revealed that the northeast-southwest trending line, considered a suture, does not separate the two different continental metamorphic basements, and that the metamorphic assemblage in the north is Precambrian in age and widely outcrops south of the suture zone(?) (Tunç et al., 2012; Yiğitbaş et al., 2014 a,b; 2018; Yiğitbaş and Tunç, 2020). The Çetmi ophiolitic mélange, considered to represent the suture zone, corresponds to different tectonostratigraphic units of different ages from Lower Cretaceous to Paleocene-Eocene in the region (Yiğitbaş et al., 2009a, 2009b).

In this context, the unit, previously mapped and described as the Çetmi ophiolitic mélange in earlier studies (Okay et al., 1990; Okay and Satır, 2000; Beccaletto, 2004; Beccaletto et al., 2005; Duru et al., 2012), which extensively outcrops around Örenli village southwest of Bayramiç (Çanakkale, Türkiye), has been studied in detail. The reason for selecting this area is the Triassic carbonates (Okay et al., 1990; Beccaletto, 2004; Beccaletto et al., 2005), defined as blocks within this unit, and to reveal whether the unit is a subduction mélange of the Intra-Pontide Ocean. The absence of the Intra-Pontide subduction mélange identified in the Biga Peninsula would indicate that the alleged suture does not exist, at least not in this region.

Here, I present a new field, zircon U-Pb age and geochemical data from the Örenli metamorphics and associated rock units and discuss their origin, stratigraphic position and tectonic setting in the light of new and published data.

2. Geological outline

The Biga Peninsula has a pre-Liassic composite metamorphic basement and covering Mesozoic to Neogene sedimentary-volcanic rocks (Figure 1A). Metamorphic basement inliers in various parts of the peninsula have been mapped in detail in previous studies (Okay et al., 1990; Duru et al., 2004; Tunç et al., 2012; Yiğitbaş et al., 2014b, 2018; Yiğitbaş and Tunç, 2020).

Yiğitbaş and Tunç (2020) grouped these pre-Jurassic basement rocks under three tectonostratigraphic units: 1) the Kazdağ Unit, 2) the Kalabak Unit, and 3) the Karakaya Unit. The Kazdag Unit crops out in the Kazdağ Massif, forms an antiformal structure plunging to the northeast, and extends from the Gulf of Edremit in the southernmost part of the Biga Peninsula. The core of this antiform is a gneiss dome that consists mainly of a Triassic island-arc assemblage (Fındıklı metamorphics), a metaophiolitic assemblage (Tozlu metaophiolite), a milky-white marble (Sarıkız marble), and gneisses and migmatites (Sütüven Formation) (Figure 2; Yiğitbaş et al., 2014a, 2018).

The Kalabak Unit, which crops out in Çamlıca, Karabiga, and Karadağ massifs, is represented by a volcanic arc and continental margin assemblages of Precambrian-Early Paleozoic age, cut by metagranites of Early Devonian age (Tunç et al., 2012; Yiğitbaş and Tunç, 2020), and overlies the Kazdağ Unit with a tectonic contact (Figures 1B and 2). These are unconformably overlain by the rocks of the Karakaya Complex, including the units of a marginal basin that opened during the Triassic period and closed at the end of this period (Şengör and Yılmaz, 1981).

These different metamorphic assemblages are unconformably overlain by Jurassic-Cretaceous carbonate platform deposits named as the Sakarya Unit (Figure 1A and 1B; Yiğitbaş et al., 2009a; Duru et al., 2012; Yiğitbaş and Tunç, 2020). This carbonate platform sequence passes into a blocky-olistostromal unit with a matrix of sandstone, shale, greywacke, and mudstone in the north of the Gönen-Edremit line (Pontid Unit; Figure 2). The Pontid Unit, consisting of various blocks of limestone, chert, and sandstone in a sandstone-shale matrix around the type locality of Çetmi village, tectonically overlies the Kazdag Unit. On the other hand, the same unit overlies the metamorphic basement rocks with an unconformity in the Karabiga Massif. In the Şarköy (Tekirdağ, NW Türkiye) outcrops, serpentinite and blueschist blocks occur in a Paleocene-Eocene sedimentary matrix composed mainly of sandstone, marl, and conglomerate (Yiğitbaş et al., 2009a and 2009b).

This study was carried out on one of the most widely distributed outcrops of the Çetmi mélange (Figure 3), defined in the Ayvacık-Karabiga zone of Okay et al. (1990). The Çetmi mélange(?) on the northwest flank of the Kazdağ Massif is represented by a low-grade metamorphic assemblage, consisting of metavolcanic, metasedimentary rocks and recrystallized limestones in the study area. Since these units are composed of different lithologies, they have been mapped as the Çetmi mélange (Okay et al., 1990; Okay and Satır, 2000; Beccaletto, 2004; Beccaletto et al., 2005; Duru et al., 2007), and the (recyristallized) limestones, defined as the blocks within this mélange, and all limestones in the study area are considered Triassic-

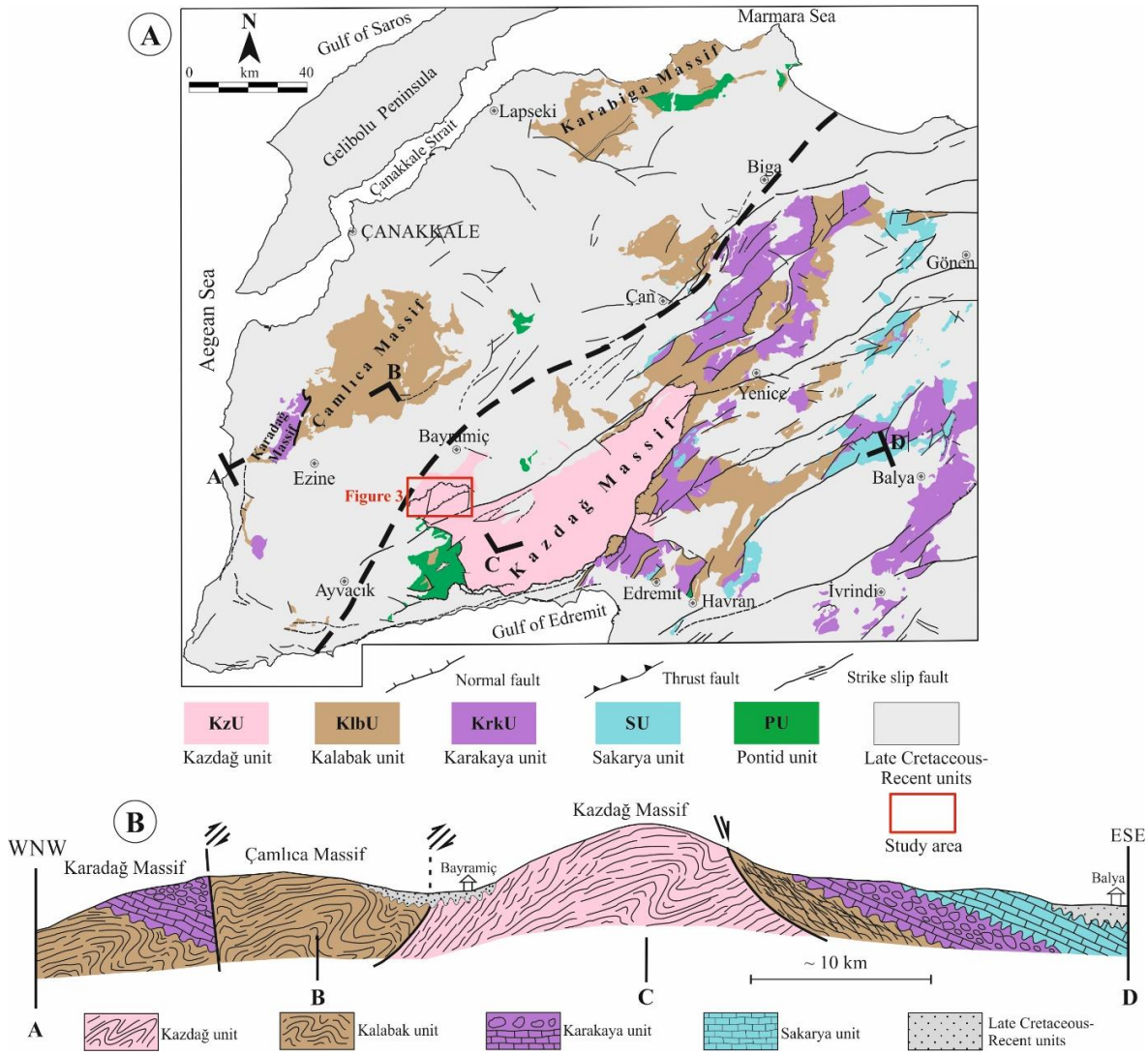

Figure 1. A) Geological map showing the main tectonostratigraphic units in the Biga Peninsula (Yiğitbaş and Tunç, 2020). The black dashed line shows the zone referred to as the Intra-Pontide suture in previous studies. **B)** Composite geological cross-section, showing the tectonostratigraphic relationships of the metamorphic units in the Biga Peninsula. (The cross-section is simplified and generalized in order to show the relations on a plane and therefore does not show some details of the section line on the geological map in Figure 1A).

aged, and the unit in which they are found (matrix of the mélange) is considered to be younger (Okay et al., 1990). However, these lithologies form a laterally and vertically transitional succession with a recognizable internal order, despite the low-grade metamorphism.

In this paper, the low-grade metamorphic rocks of the Örenli metamorphics, which were previously mapped and defined as the subduction mélange of the Intra-Pontide Ocean (*i.e. Çetmi mélange*; Okay et al., 1990; Okay and Satır, 2000; Beccaletto, 2004; Beccaletto et al., 2005; Duru et al., 2012), a mylonitic zone (*i.e. Alakeçi mylonite zone*; Okay et al., 1990; Bonev and Beccaletto, 2007; Bonev et al., 2009; Cavazza et al., 2009) and/or the Karakaya Complex (Duru et al., 2007), were remapped and new geochemical and geochronological data are presented here to draw conclusions as to the tectonostratigraphic evolution of the region.

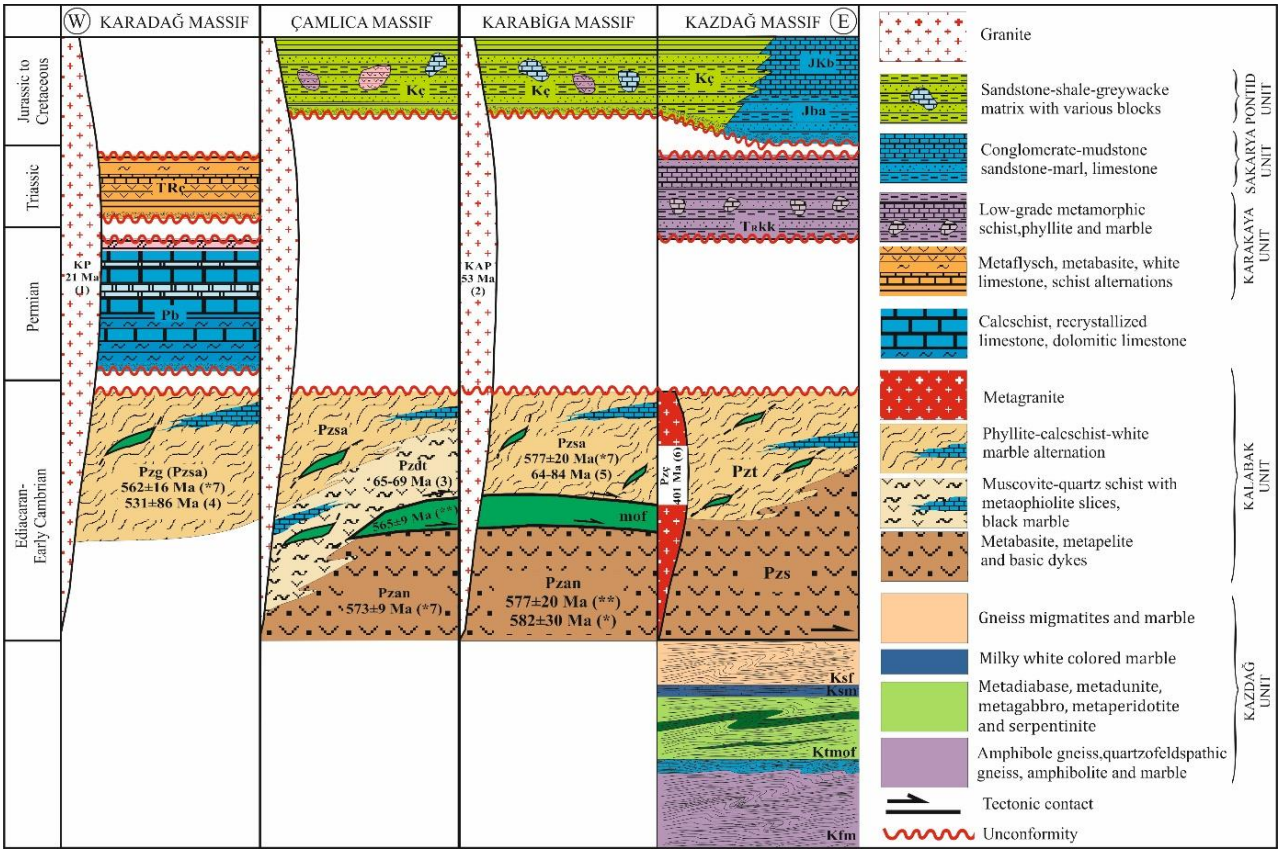

Figure 2. Correlation of metamorphic rocks, outcropping in different areas under Tertiary volcanic-sedimentary cover in the Biga Peninsula (Tunç et al., 2012; Yiğitbaş et al., 2014a). This tectonostratigraphic correlation shows that a significant part of the metamorphic rocks can be correlated with each other. (**Kfm:** Fındıklı metamorphics, **Ktmof:** Tozlu metaophiolite, **Ksm:** Sarıkız marble, **Ksf:** Sütüven Formation, **Pzan:** Andıktaşı Formation, **Pzs:** Sazak Formation **Pzdt:** Dedetepe Formation, **Pzsa:** Salihler Formation, **Pzg:** Geyikli Formation, **Pzt:** Torasan Formation, **mof:** metaophiolite, **TRkk:** Karakaya Complex, **TRç:** Çamköy Formation, **Jba:** Bayırköy Formation, **JKb:** Bilecik limestone, **Kç:** Çetmi group, **KP:** Kestanbol pluton, **KAP:** Karabiga pluton, **Pzç:** Çamlık metagranite. (*) maximum sedimentation age of the protolith, (**) cyrstallization age of the protolith. **1)** Birkle and Satır, (1995); **2)** Beccaletto et al. (2007); **3)** Okay and Satır (2000) -Rb-Sr (phengite-whole rock); **4)** Duru et al. (2012) -Rb-Sr (muscovite-whole rock); **5)** Aygül et al. (2012) -Rb-Sr (phengite-whole rock); **6)** Aysal et al. (2012) - U-Pb zircon; and **7)** Tunç et al. (2012) -U-Pb zircon).

The metamorphic rocks outcropping in the study area are: 1) the Kazdağ Unit, 2) Akpınar serpentinite, and 3) Örenli metamorphics (Figure 3). Since the main subject of this study is the Örenli metamorphics, other tectonostratigraphic units will be described only in general terms, and the focus will be on the Örenli metamorphics.

The Kazdağ Unit is represented by high-grade metamorphic schist-amphibolite-granitic gneiss alternations and milky white marble lenses of the Sütüven Formation in the southeast parts and constitutes the basement of the study area (Tunç, 2008).

The Akpınar serpentinite, which was named by Tunç (2008) for the first time, contains lisvenite-magnesite occurrences in places, and most of them are serpentinized from ultramafic rocks. It also contains metagabbro-amphibolite levels in some parts. These ophiolitic rocks, previously evaluated within the Çetmi mélange, are individual tectonic slices with a thickness of about 2 km, and tectonically underline the Örenli metamorphics (Tunç, 2008; Figure 3 and 4).

The contact between the rocks of the Kazdağ Unit, the rocks of the Örenli metamorphics and the serpentinite tectonic slice (Akpınar serpentinite), is a right-lateral strike-slip fault (Bıçkıdere fault) which has a vertical component (Figures 3 and 4).

The Örenli metamorphics, which was mapped and named for the first time by Tunç (2008), is mainly composed of low-grade metamorphic volcanic and sedimentary rocks. This succession contains large crystalline and milky white marble blocks of various sizes in the east-southeast parts of the study area (Figure 4). On the other hand, in the west-northwest parts, it does not contain any blocks,

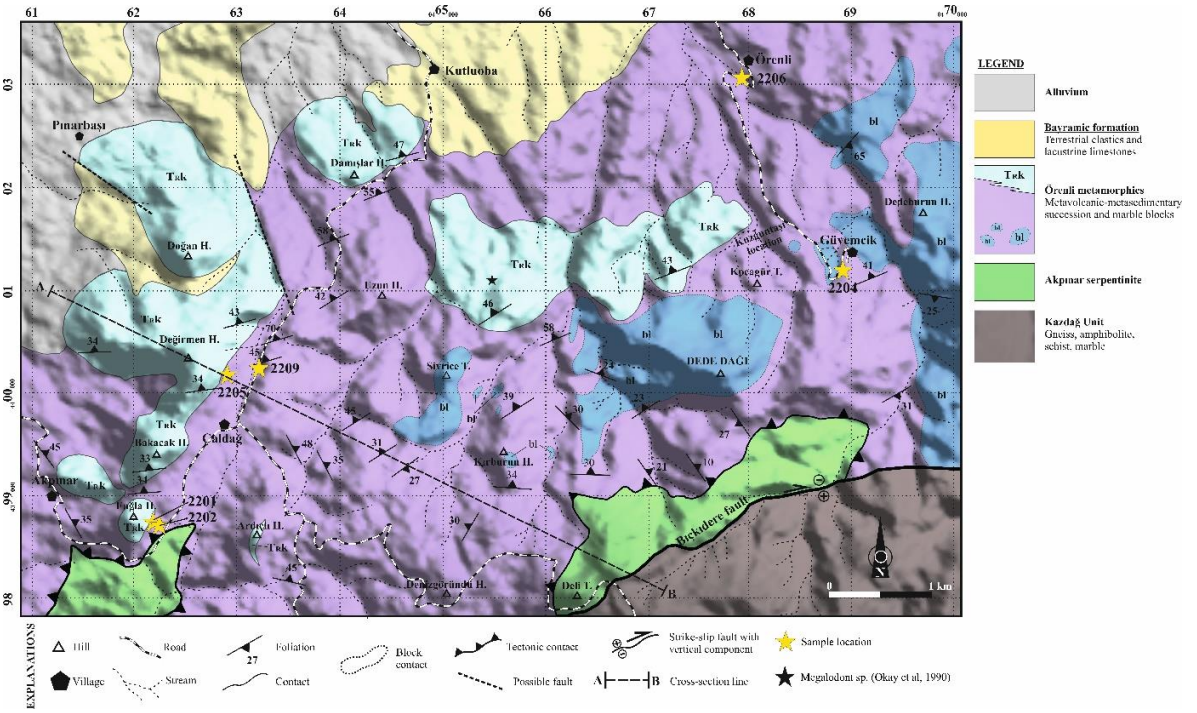

Figure 3. Geological map of the study area.

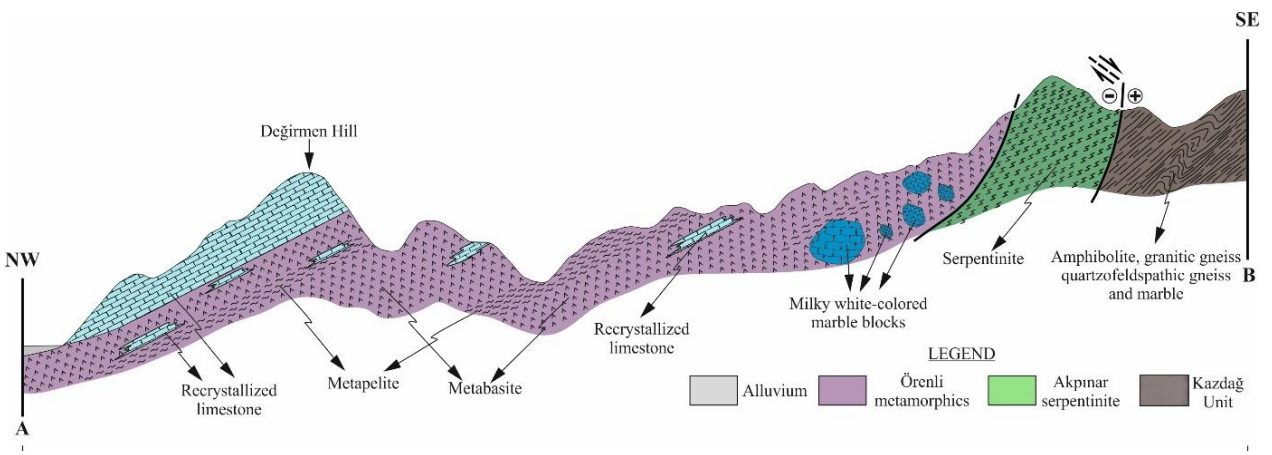

Figure 4. Northwest-southeast trending geological cross-section showing the interrelations of the units outcropping in the study area (see Figure 3 for the cross-section line).

and shows a gradual transitional primary stratigraphical relationship with the gray–light gray, microcrystalline, recrystallized limestones (Figure 4).

Metavolcanic rocks, which form the most common lithology in the Örenli metamorphics, are dark green, massive, and weakly foliated. In addition to intermediate-mafic metabasites, felsic-intermediate metavolcanic rocks also crop out around Örenli village. Metasedimentary rocks, alternating with metavolcanic rocks, are yellow-light brown in their outcrops between Akpınar and Çaldağ villages, and gray-light gray in their outcrops between Çaldağ and Alakeçi villages, well-foliated and show pencil cleavage structure.

There are two types of metacarbonate in the Örenli metamorphics. The first one of these is marble blocks of various sizes (from meters to kilometers) that widely outcrop in the east-northeast parts of the study area around Güvemcik village (Figure 3). The weathered surfaces of these marbles are gray, and the fresh surfaces are milky white in color, with large calcite crystals and showing

sugar texture. The second type of (meta-) carbonates, on the other hand, is light gray on both fresh and weathered surfaces, brittle, and contains karstic surface structures in their outcrops between Akpınar-Çaldağ-Kutluoba villages in the west-southwest parts of the study area. Fresh surfaces are micritic and recrystallized in places.

Unlike the first type of marbles, the second type of carbonates preserves their primary stratigraphic relationship with the metavolcanic-metasedimentary assemblage and constitutes the structurally and stratigraphically uppermost levels of the sequence (Figure 5). Okay et al. (1990) named these micritic limestones as Sakarkaya limestone and suggested they were of Late Triassic age, based on the *Megalodont* fossils. Beccaletto (2004) and Beccaletto et al. (2005) also suggested a Late Triassic age for the same micritic limestones in the southwest of Akpınar village (from an outcrop outside the map area in Figure 3), based on foraminiferal fossils (*Glomospirella expansa*, *Triasina hantkeni*, *Aulotortus gr. sinuosis*, *Endotebanella Kocaliensis*, *Auloconus permodiscoides*, *and Nodosariidae*), compatible with Okay et al. (1990).

The primary relationship of metavolcanic-metasedimentary rocks and recrystallized limestone is very well seen between the Fuğla and Bakacak hills when walking towards Bakacak Hill by following the paths towards the north (UTM Coordinates: 35S 0462032 E / 4399076 N; Figure 6). Towards the peak of Bakacak Hill, this succession, where foliation planes are compatible with each other (N80E/34NW), passes upward into light gray and slightly recrystallized limestones, which constitute the structurally and the stratigraphically uppermost levels of the succession all over this area, with a distinct layer alternation towards the top.

To the east of Fuğla Hill and on the southern slopes of Bakacak Hill, this metavolcanic-metasedimentary-recrystallized limestone succession is cut by dark

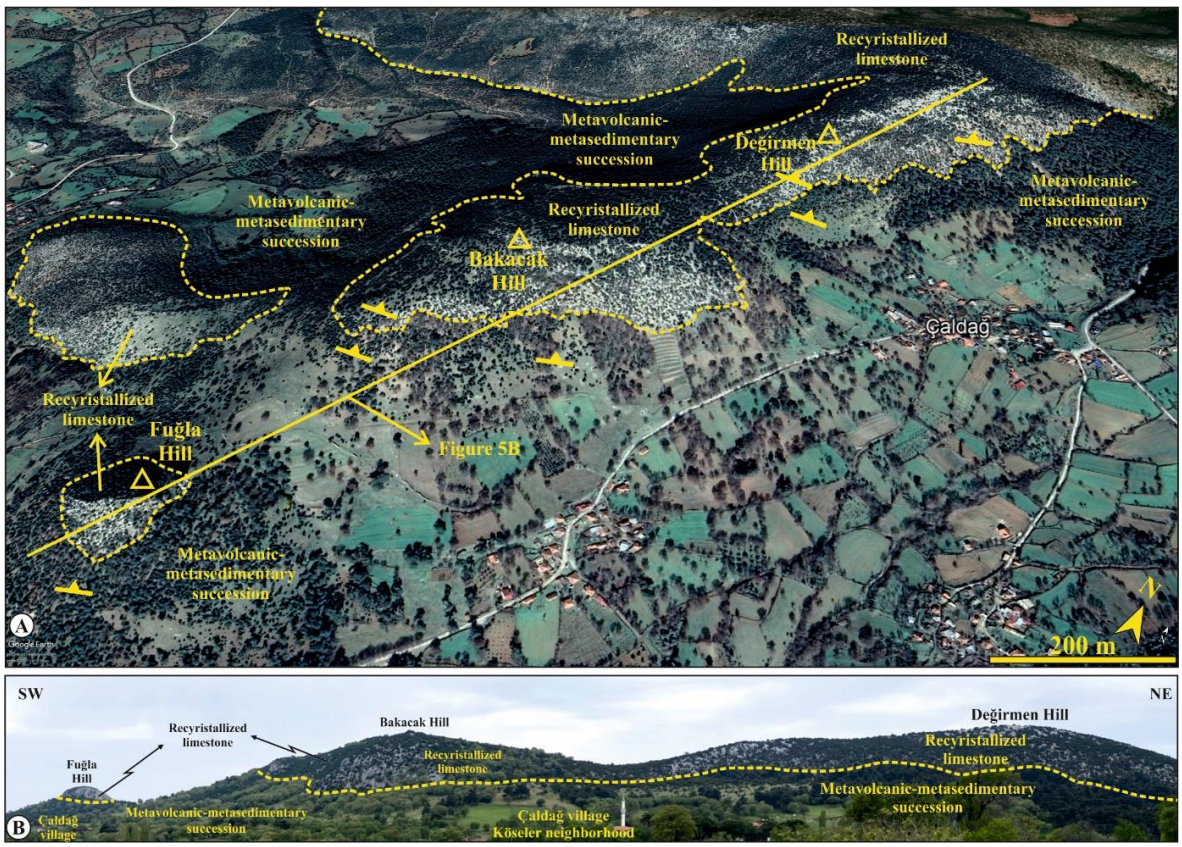

Figure 5. A) Google Earth image of metavolcanic-metasedimetary alternation and recrystallized limestones wedging and forming lenses in all scales in the Fuğla, Bakacak, and Değirmen hills west of Çaldağ village. In this part of the study area, the regular carbonate sequence is always on the top of the metavolcanic-metasedimentary sequence (yellow line passing through Fuğla, Bakacak, and Değirmen hills shows the direction of the panoramic photograph in Figure 5B). **B)** Panoramic photograph showing the relationship between the recrystallized limestones cropping out at Fuğla, Bakacak, and Değirmen hills and the metavolcanic-metasedimentary sequence.

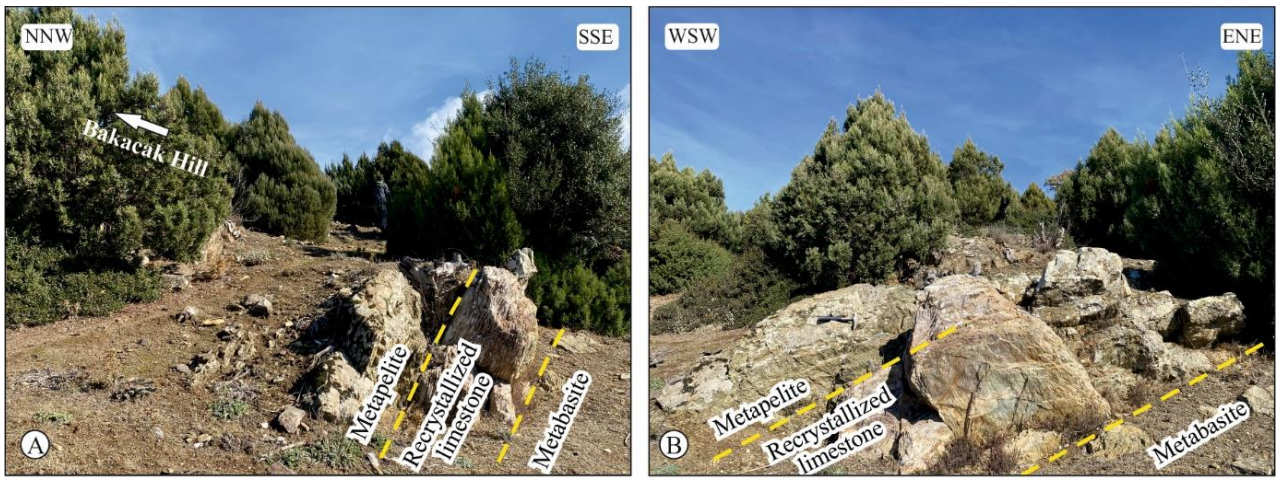

Figure 6. A) Photograph showing the metavolcanic-metasedimentary rocks and recrystallized limestone alternation on the southern slope of Bakacak hill (UTM Coordinates: 35S 0462032 E / 4399076 N). Their foliation planes are compatible with each other. **B)** Looking at the same outcrop from south to north.

green-black diabase dykes (Figure 7A), which includes recrystallized limestone enclaves (Figure 7B).

The Bayramiç Formation (Late Miocene; Tekkaya, 1973), outcropping in the northern parts of the study area (Figure 3), starts with a not very thick basal conglomerate around Kutluoba village and north of Pınarbaşı village and passes upward into terrestrial clastics and lacustrine limestones. It unconformably overlies the Örenli metamorphics and is unconformably covered by alluvium.

3. Analytical techniques

A total of five representative metavolcanic rock samples were selected for geochemical analyses. Major oxides and trace-rare earth elements were analyzed by using inductively coupled plasma-atomic emission spectroscopy (ICP-AES) and inductively coupled plasma-mass spectrometry (ICP-MS) methods, at the ALS Chemex laboratory in Canada, followed by lithium metaborate/tetraborate fusion and dilute nitric digestion. Geochemical diagrams were prepared using Geochemical Data Toolkit (GCDkit) software (Janoušek et al., 2006). The zircons were extracted from the sample using conventional mineral separation techniques including crushing, sieving, and magnetic and heavy liquid separation at the Mineral Separation Laboratory of the Çukurova University Geological Engineering Department. The extracted zircon grains were mounted in cold resin prior to grinding and polishing. The CL images were taken at Hacettepe University Central Research Laboratories (HUNITEK). The zircons were analyzed using an ESI NWR213 Nd:YAG laser attached to a Perkin-Elmer Nexion 2000P ICP-MS at the Çukurova University Central Research Laboratory.

The data acquisition includes a 20-s background measurement followed by a 30-s sample ablation. The laser was used in single spot mode with 25–40 µm spot size at 6–7 J/cm^2 energy with a 10-Hz repetition rate. He gas was used to carry the ablated material to the ICP-MS. The ICP-MS was used in time-resolved mode and was calibrated using the standard glass NIST SRM 612 to obtain the maximum U+ signals with a ThO/Th ratio of ≤ 0.5%. Ar gas was used for the plasma gas. During the analyses, ^{204}Pb, ^{206}Pb, ^{207}Pb, ^{208}Pb, ^{232}Th, ^{235}U, and ^{238}U isotopes were measured at 10 ms, 10 ms, 40 ms, 40 ms, 10 ms, 10 ms, 10 ms, 10 ms, respectively. The zircon 91500 (Wiedenbeck et al., 2004) was used for the primary reference and the Plesovice reference zircon (Sláma et al., 2008) was used as unknown within the sample batch to test the accuracy and external reproducibility. The Iolite v4 is used for data reduction and processing (Paton et al., 2011).

4. Analytical results

4.1. Geochemistry

Five samples were collected from the metavolcanic rocks of the Örenli metamorphics in order to determine the sources of these rocks and the tectonic environments in which they were formed (See Figure 3 for sample locations). The whole-rock major oxides and the trace and rare earth element analysis results of representative samples are given in Appendix 1.

The SiO_2 and K_2O content of the metavolcanic samples have a wide range (41.07%–69.28%; and 1.17%–6.74%, respectively). Metavolcanic samples are characterized by medium-high Al_2O_3 (14.79%–28.8%), low MgO (1.75%–7.50%), low-medium Cr (12.25–298.83 ppm) and low-

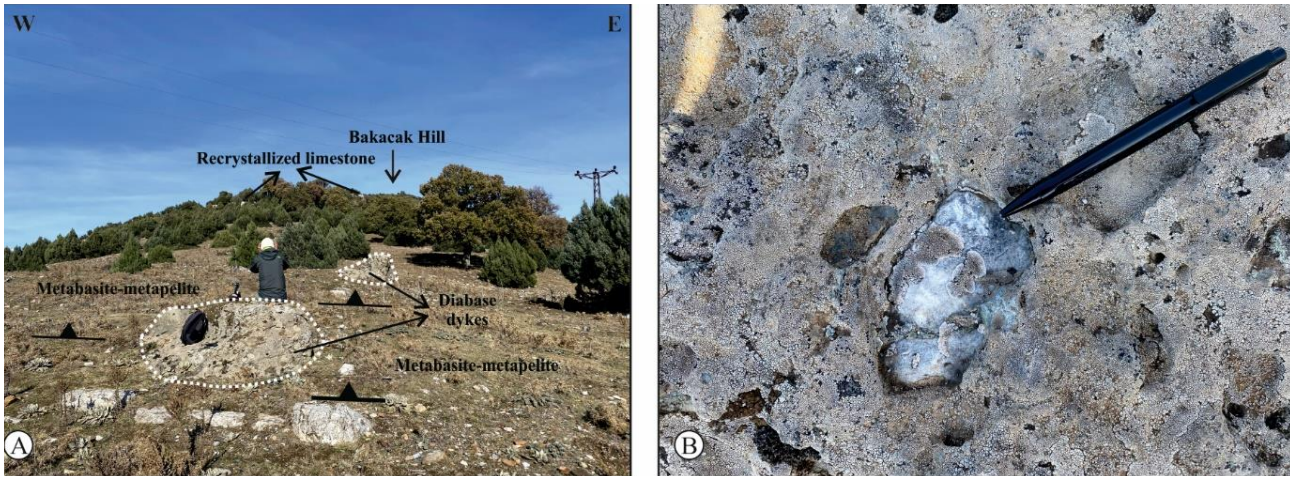

Figure 7. A) Outcrops of diabase dykes observed on the southern slope of Bakacak Tepe (UTM Coordinates: 35 S 0462049 E / 4398992 N). **B)** Recrystallized limestone enclave in these diabase dykes.

medium Nb (4.90–15.03 ppm) values. The increased Na_2O (0.11–5.14%) values in some samples must be due to the crystallization of albite and alteration during low-grade metamorphism.

The calc-alkaline association of the Basalt-Andesite-Dacite-Rhyolite (BADR) pattern is seen in the metavolcanic samples in the SiO_2 versus Zr/TiO_2 classification diagram (Figure 8; Winchester and Floyd, 1977), which is the signature volcanic rock suite of convergent margins (Perfit et al., 1980; Grove and Kinzler, 1986).

When 5 metavolcanic rock samples are plotted to the AFM [A: ($Al_2O_3 - 3K_2O$); F: ($FeO - TiO_2 - Fe_2O_3$); and M: (MgO)] diagram, suggested by Irvine and Baragar (1971), and the Ti/100 – Zr – 3Y (ppm) diagram, suggested by Pearce and Cann (1973), it is seen that all the samples fall into the calc-alkaline area, (Figures 9A and 9B).

Rare earth elements (REE) are known to be the least mobile elements during hydrothermal alteration and low-grade metamorphism (Michard, 1989; Peate, 1997). Therefore, REE diagrams normalized to chondrite provide important information about the source and the crystallization evolution of magma. The REE spider diagram normalized to chondrite (normalizing values are taken from McDonough and Sun, 1995) shows that these rocks are enriched with light rare earth elements (LREE) when compared to heavy rare earth elements (HREE) (Figure 10A). The $(La/Y)_{cn}$ ratio is between 3.42 and 7.74.

The Eu anomaly is controlled mainly by feldspars in rocks. Therefore, removal of feldspar from the melt by crystallization or partial melting of the rock ultimately causes a negative Eu anomaly in the melt (Rollinson, 1993). Eu anomalies [$(Eu/Eu^*)_{cn}$] of metavolcanic samples are between 0.48 and 0.98. The mid-oceanic ridge basalts (MORB) normalized multielement spider diagram (normalizing values are taken from McDonough and Sun, 1995) shows that, while the compatible elements and the high field strength (HFS) elements on the right side of the diagram have a ratio and pattern compatible with MORB, a significant enrichment is observed in terms of incompatible elements and large ion lithophile (LIL) elements (Figure 10B). All the metavolcanic samples show a significant negative Nb and Ti anomaly. LIL elements are highly mobile in aqueous fluids. Therefore, the differentiation functions accompanying the greenschist facies metamorphism affect the amount of these elements. Strong negative Nb, Zr, and Hf anomalies in metavolcanic rocks on active continental margins indicate a continental contamination at the source of these elements. This continental impact may be related either to partial melting at the base of the continental crust or to the contamination of mafic magma with continental material. Indeed, in addition to the remarkable negative Nb anomaly in all metavolcanic samples in the study area, a considerably higher enrichment in all incompatible elements is seen compared to the volcanic arc tholeiites. In addition to the enrichment patterns in LREEs and the incompatible elements and negative Nb anomaly relative to HREEs, the negative Ti anomaly indicates that these rocks characterize high-K calc-alkaline volcanism at active continental margins (Wilson, 1989; Gill, 2010 and references therein). The metavolcanic rocks were also evaluated in the tectonic discrimination diagrams (Figure 11). Diagrams to be used for this purpose were selected from immobile elements during alteration and metamorphism. Mobile elements, such as Na, K, Ca, Ba, Rb, Sr, and LREEs, do not provide the expected benefit when used for tectonomagmatic discrimination. Therefore, relatively immobile elements were preferred, such as Fe, Ti, Ni, Cr, V, Zr, Nb, Ta, and Hf.

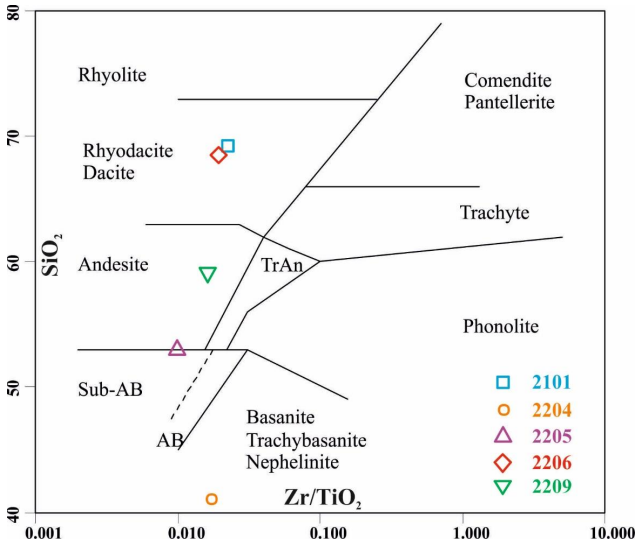

Figure 8. SiO_2 versus Zr/TiO_2 (Winchester and Floyd, 1977) classification diagram of the metavolcanic rocks in the Örenli metamorphics.

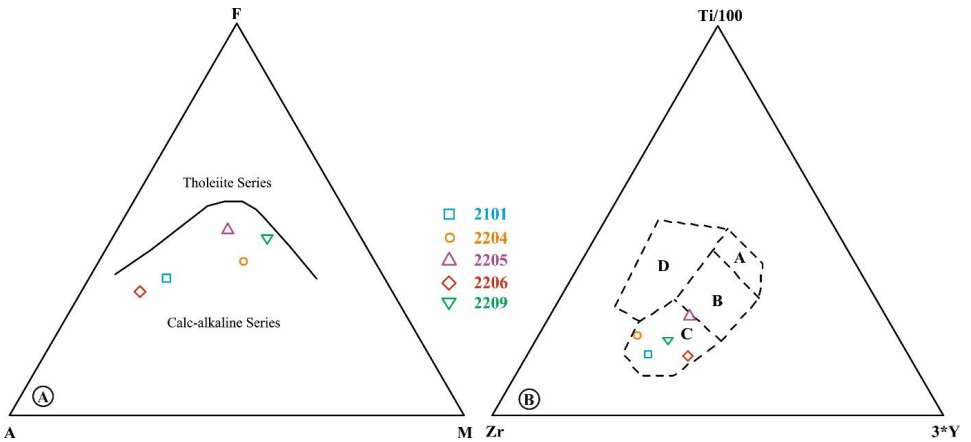

Figure 9. Distribution of metavolcanic samples of the Örenli metamorphics in **A)** AFM diagram (Irvine and Baragar, 1971), and **B)** Ti/100 - Zr - 3Y (ppm) diagram (Pearce and Cann, 1973) (Abbreviations: A: IAT= island arc toleyite, field B: MORB+VAB= mid-ocean ridge basalt+volcanic arc basalt. C: CAB= calcalkaline basalt, D: WPB= intraplate basalt).

Comparison of trace elements in bivariate diagrams for subduction-associated basalts is very useful in separating mantle components from subduction-related components in magma petrogenesis (Pearce, 1982).

Metavolcanic samples of Örenli metamorphics were evaluated in the Th/Nb versus La/Yb diagram suggested by Hollocher et al. (2012) (Figure 11A), as well as the Ti (ppm) versus Zr (ppm) diagram suggested by Pearce (1982) (Figure 11B). Accordingly, all metavolcanic samples fall into the continental arc and island arc volcanic areas (Figure 11).

4.2. Geochronology

Sixty zircon grains picked from the diabase dyke sample, which cuts the metavolcanic-metasedimentary succession of the Örenli metamorphics, were analyzed, and 33 of them gave concordant results in the range of 90%–110%. The investigated zircon grains yielded concordant results; they have 1:1–2:1 length–width ratios and are rounded, subrounded, or semieuhedral, and show oscillatory zoning. The size of the zircon grains ranges from approximately 50 µm to 200 µm (Figure 12), and the Th/U ratios of the concordant results range from 0.295 to 1.047 (Appendix 2).

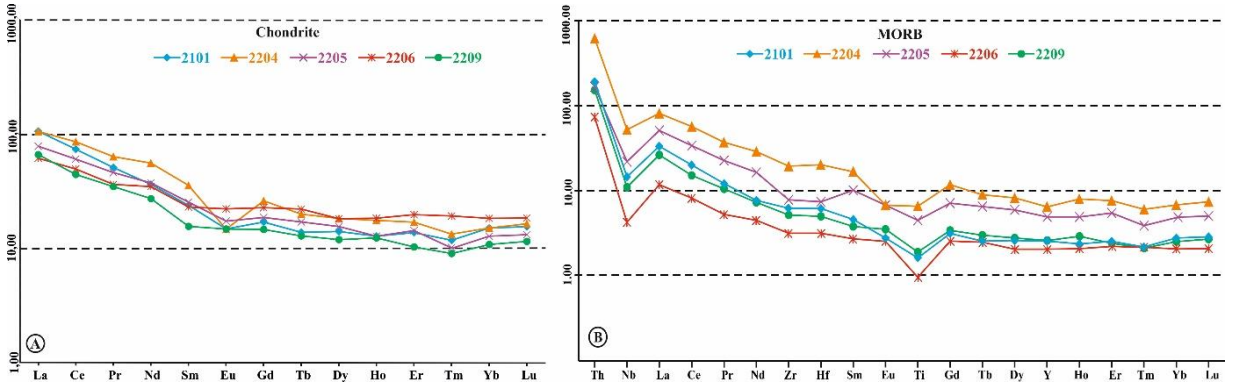

Figure 10. Rare earth element variation (spider) diagrams of metavolcanic rock samples **A)** normalized to chondrite, **B)** normalized to MORB.

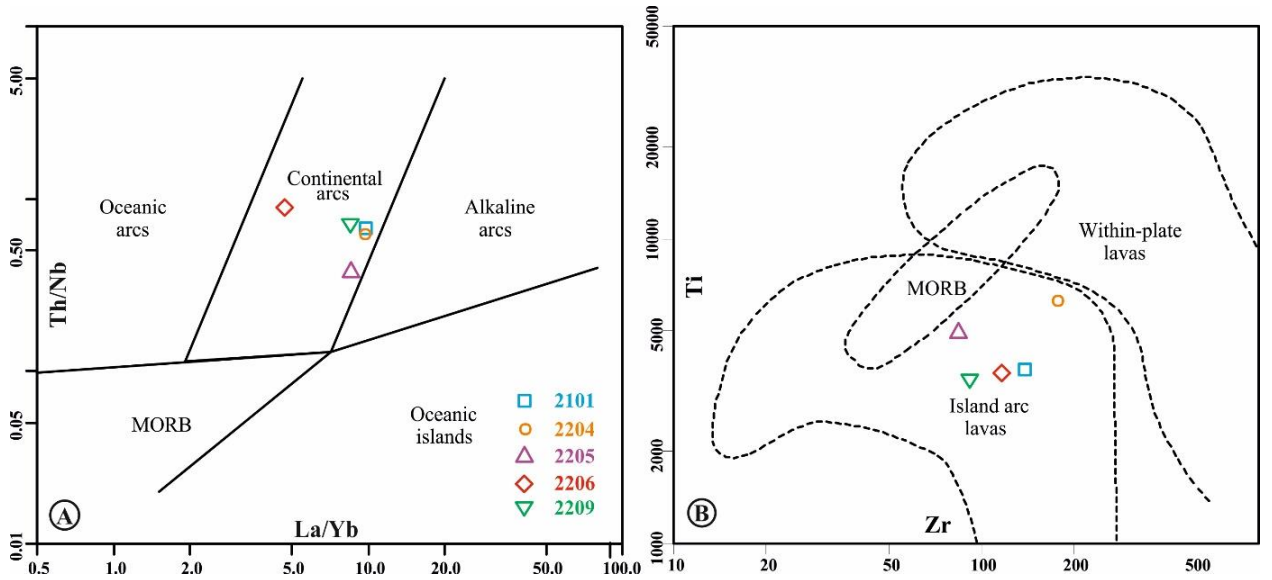

Figure 11. Distribution of metavolcanic samples of the Örenli metamorphics in **A)** Th/Nb – La/Yb (Hollocher et al., 2012) and **B)** Zr – Ti (Pearce, 1982) tectonic discrimination diagrams.

Results of the LA-ICP-MS zircon U-Pb analysis of the diabase sample (2202) are shown in concordia (Figure 13A) with the combined frequency and probability density diagrams (Ludwig, 2003; Figure 13B). The crystallization age of the diabase sample is 165.81 ± 1.55 Ma.

Unfortunately, the number of zircons giving their age could not be obtained in the metavolcanic rock samples. However, as stated in the Geological Outline section, metavolcanic-metapelitic rocks are transitional with the Triassic recrystallized limestones at the top of the succession. In this case, the 165.81 ± 1.55 Ma age, taken from the dykes cutting this succession, supports our field observations.

5. Discussion

The Örenli metamorphics, which have been mapped and named the Çetmi mélange, Alakeçi Mylonite Zone, and/or Karakaya Complex in previous studies (Okay et al., 1990; Beccaletto, 2004; Beccaletto and Jenny, 2004; Beccaletto et al., 2005, 2007; Bonev and Beccaletto, 2007; Bonev et al., 2009; Cavazza et al., 2009; Duru et al., 2007, 2012), have been mapped in detail on the northern flank

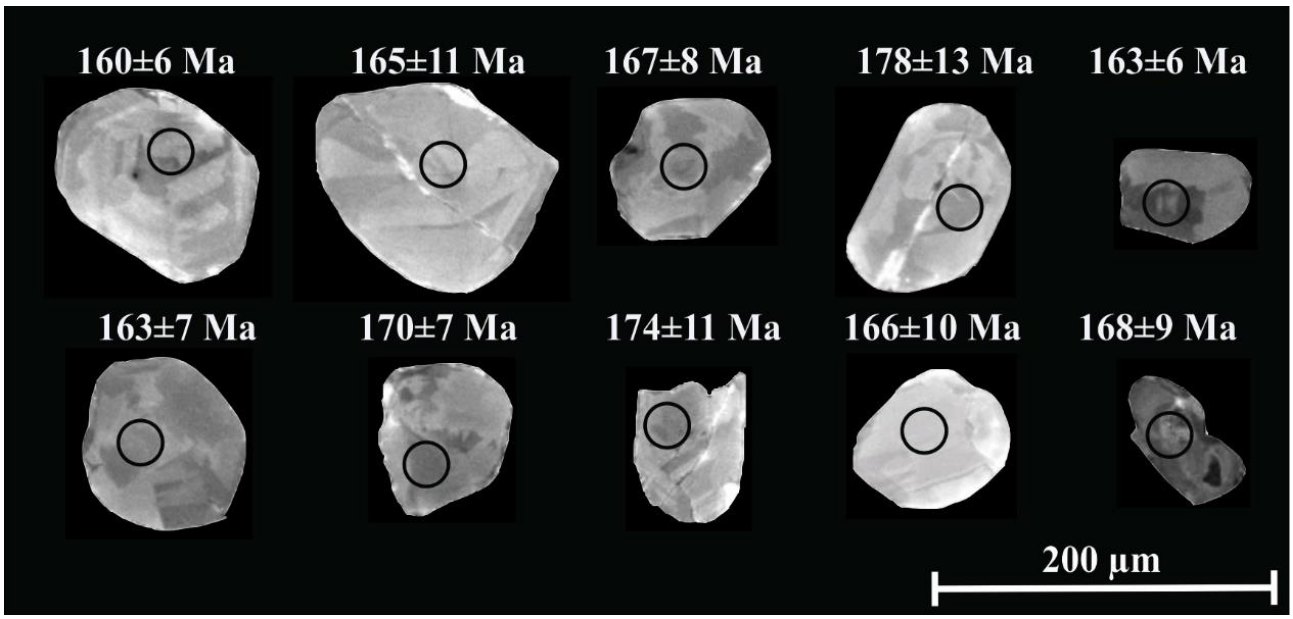

Figure 12. Cathodoluminescence (CL) images of representative zircon grains from the diabase dyke sample (2202), cutting the metavolcanic rocks of the Örenli metamorphics, showing their internal structure, the location of laser spots, and ages with 2-sigma-error in Ma

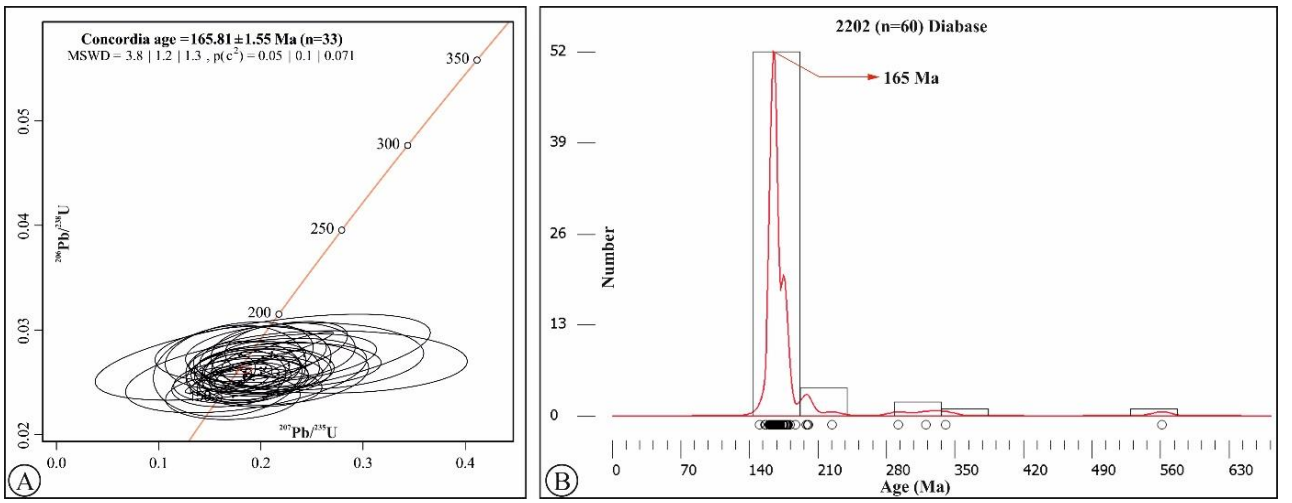

Figure 13. A) Concordia diagram of sample 2202 (diabase) taken from the eastern slope of Fuğla Tepe (UTM Coordinates: 35 S 0462049 D - 4398703 N), and **B)** Combined frequency and probability density diagram showing the distribution of zircon ages.

of the Kazdağ Massif, in the area between Akpınar-Çaldağ-Kutluoba-Örenli villages, south of Bayramiç (Çanakkale, Türkiye), where they best crop out (Figure 3). Despite the polyphase deformation and low-grade metamorphism, the stratigraphic position (primary layering) of the Örenli metamorphics can be determined by the metavolcanic-metapelite alternation in this area. The tectonostratigraphically lowermost levels of the Örenli metamorphics crop out in the east-southeast parts of the study area. In this part of the study area, metavolcanic and metapelite alternation of the unit contains milky white marble blocks varying from meters to kilometers in size in the area between Örenli and Güvemcik villages (Figures 3 and 4). No blocks other than marble were found in the unit. This shows that there are marbles directly in the source area of the Örenli metamorphics. The closest unit in the region resembling these white and coarse crystalline marbles is the Sütüven Formation in the Kazdağ Unit (Figure 2).

5.1. The age of the Örenli metamorphics

The tectonostratigraphically uppermost levels of the Örenli metamorphics crop out in the west-northwest parts of the study area. In this area, the primary layering of the unit, which is characterized by a metapelite-metabasite succession, generally strikes to NE and dips to NW (Figures 3 and 4). These metavolcanic-metasedimentary rocks gradually pass upward into recrystallized limestones in the upper levels of the unit. This transition is best seen at the western end of the limestone outcrop on Bakacak Hill (UTM Coordinates: 35S 0462032 E / 4399076 N). Okay et al. (1990), Beccaletto (2004), and Beccaletto et al. (2005) obtained a Late Triassic fossil age from these carbonate outcrops. According to this fossil age and the field relationships of the metavolcanic-metapelite sequence and carbonates, the Örenli metamorphics must also be Triassic in age, and the milky white marble blocks must have been derived from an older basement.

The diabase dykes cutting the metavolcanic-metasedimentary rocks of the Örenli metamorphcs yield a zircon U-Pb age of 165.81 ± 1.55 Ma. This age also supports the observation that the metavolcanic-metapelite sequence is covered by Late Triassic limestones. According to all these stratigraphic and geochronological data, the Örenli metamorphics must be Triassic in age.

5.2. Tectonic setting of the Örenli metamorphics

The calc-alkaline association of the Basalt-Andesite-Dacite-Rhyolite (BADR) pattern, which is the signature volcanic rock suite of convergent margins (Perfit et al., 1980; Grove and Kinzler, 1986), is seen in the metavolcanic samples in the chemical classification diagram (Figure 8). In addition, the geochemical composition of all the volcanic rock samples shows an active continental margin and continental volcanic arc environment in the tectonic discrimination diagrams (Figure 11). The fact that the lower levels of the unit contain marble blocks and that it is underlain by an ophiolite slice with a tectonic contact supports the characteristic of an active continental margin. Okay and Monié (1997) found Triassic eclogite tectonic slices to the east of Bandırma in northwestern Türkiye, which they believe to be related to the Paleo-Tethyan subduction, and this also supports the active continental margin idea. It has been previously stated that the Tozlu metaophiolite located in the Kazdağ Massif, just south-southeast of the study area, is remnants of the Paleo-Tethys Ocean (Yaltırak and Okay, 2004; Erdoğan et al., 2013). The metaophiolite slice (Akpınar serpentinite), tectonically underlying the Örenli metamorphics, is probably the equivalent of the Tozlu metaophiolite (Figure 14).

The geochemical characteristics of the Örenli metamorphics show that these rocks developed near a continental volcanic arc system, related to the subduction of the Paleo-Tethys oceanic lithosphere, most probably in the fore-arc environment, and were later pushed onto the ophiolite and gained its present position (Figure 15).

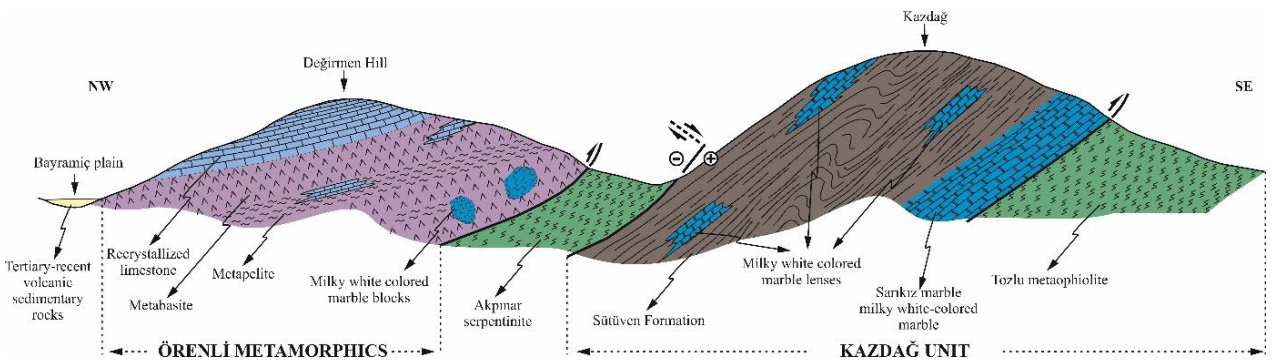

Figure 14. Sketch cross-section showing the relationship between the Örenli metamophics and the Kazdağ unit.

6. Conclusions

1. The Örenli metamorphics, which were evaluated as a subduction accretionary mélange of the Intra-Pontide Ocean in previous studies, are a regular succession consisting of low-grade metamorphic volcanic and sedimentary rocks.
2. These metavolcanic and metasedimentary rocks present a horizontal and vertical transitional and primary contact relationship with Triassic (Okay et al., 1990; Beccaletto, 2004; Beccaletto et al., 2005) recrystallized limestones, and are cut by Mid-Jurassic (165.81 ± 1.55 Ma) diabase dykes. According to this, the age of the unit is Triassic.
3. Geochemical data of metavolcanic rocks show that these rocks represent an active continental margin.
4. All data indicate that the Triassic Örenli metamorphics cannot be considered remnants of the Intra-Pontid Ocean.

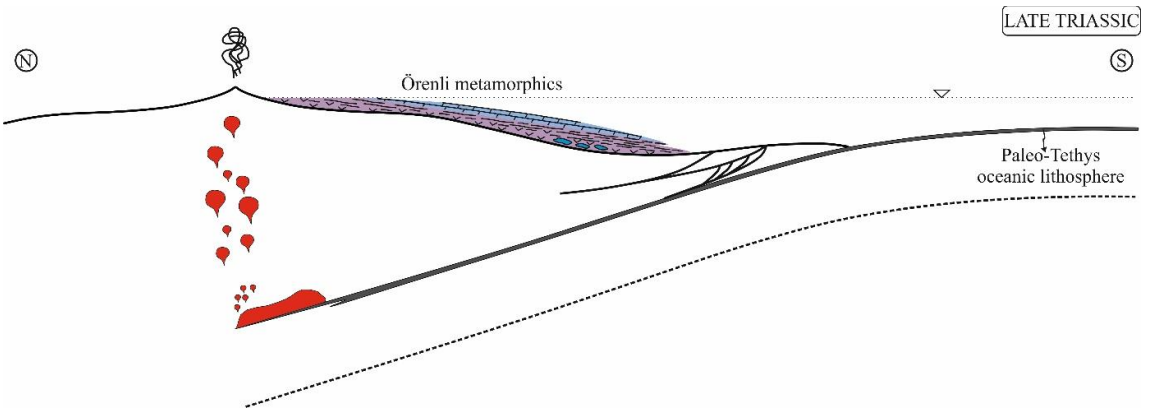

Figure 15. Paleogeographic reconstruction of the active continental margin of the Paleo-Tethys Ocean and the associated volcanic arc and fore-arc basin during the Upper Triassic period.

Acknowledgments
This study was supported by TÜBİTAK (Project number 121Y089). I would like to express my sincere thanks to Prof. Dr. Erdinç Yiğitbaş for his help at every stage of this study. I would like to thank Semih Gildir for his help during geochronological studies, and Prof. Dr. Osman Candan for his help with the thin sections. The Editor and reviewers are thanked for their constructive and valuable comments and suggestions.

References

Aygül M, Topuz G, Okay Aİ, Satır M, Meyer HP (2012). The Kemer metamorphic complex (NW Turkey): A subducted continental margin of the Sakarya Zone. Turkish Journal of Earth Sciences 21 (1): 19–35. https://doi.org/10.3906/yer-1006-14

Aysal N, Ustaömer T, Öngen S, Keskin M, Köksal S et al. (2012). Origin of the earlymiddle Devonian magmatism in the Sakarya Zone, NW Turkey: Geochronology, geochemistry and isotope systematics. Journal of Asian Earth Sciences 45: 201-222. https://doi.org/10.1016/j.jseaes.2011.10.011

Beccaletto L (2004). Geology, Correlations and Geodynamic Evolution of the Biga Peninsula (NW Turkey). PhD, Mém. Géol. (Lausanne), no 43, 146 pp.

Beccaletto L, Jenny C (2004). Geology and Correlations of the Ezine Zone: a Rhodope Fragment in NW Turkey. Turkish Journal of Earth Sciences 13 (2): 145-176.

Beccaletto L, Bartolini AC, Martini R, Hochuli PA, Kozur H (2005). Biostratigraphic data from the Cetmi Melange, northwest Turkey: Palaeogeographic and tectonic implications. Palaeogeography, Palaeoclimatology, Palaeoecology 221 (3-4): 215-244. https://doi.org/10.1016/j.palaeo.2005.02.011

Beccaletto L, Bonev N, Bosch D, Bruguier O (2007). Record of a Palaeogene syncollisional extension in the North Aegean Sea: Evidence from the Kemer micaschists (NW Turkey). Geological Magazine 144 (2): 393-400. https://doi.org/10.1017/S001675680700310X

Bingöl E, Akyürek B, Korkmazer B (1973). Geology of the Biga Peninsula and some characteristics of the Karakaya Formation. 50th Anniversary of Turkish Republic, Congress of Earth Sciences, pp. 71.

Birkle P, Satır M (1995). Dating, geochemistry and geodynamic significance of the Tertiary magmatism of the Biga Peninsula, NW-Turkey. In: Geology of the Black Sea region. Proceedings of the International Symposium on the Geology of the Black Sea Region, Ankara, Turkey, pp. 171-180.

Duru M, Pehlivan Ş, Şentürk Y, Yavaş F, Kar H (2004). New results on the lithostratigraphy of the Kazdağ Massif in Northwest Turkey. Turkish Journal of Earth Sciences 13 (2): 177-186.

Duru M, Pehlivan Ş, Ilgar A, Dönmez M, Akçay AE (2007). Geological Map of the Bandırma-H18 Quadrangle 2007, 1:100,000 Scale. General Directorate of the Mineral Research and Exploration (MTA), Ankara, Türkiye (in Turkish).

Duru M, Pehlivan Ş, Okay Aİ, Şentürk Y, Yavaş F et al. (2012). Biga Yarımadasının Tersiyer Öncesi Jeolojisi, M.T.A. Özel Yayınlar Serisi, No 28: 7-74 (in Turkish).

Erdoğan B, Akay E, Hasözbek A, Satır M, Siebel W (2013). Stratigraphy and tectonic evolution of the Kazdağı Massif (NW Anatolia) based on field studies and radiometric ages. International Geology Review 55 (16): 2060-2082. https://doi.org/10.1080/00206814.2013.818756

Eroskay SO (1965). Paşalar Boğazı-Gölpazarı sahasının jeolojisi. İstanbul Üniversitesi Fen Fakültesi Mecmuası, 30 (3-4): 135-170 (in Turkish).

Genç Ş (1993). İznik-İnegöl (Bursa) arasındaki tektonik birliklerin jeolojik ve petrolojik incelenmesi. PhD, İstanbul Teknik Üniversitesi, Fen Bilimleri Enstitüsü, 521 p. (in Turkish).

Gill R (2010). Igneous Rocks and Processes: A Practical Guide. J. Wiley, Chichester, 428 pp.

Hollocher K, Robinson P, Walsh E, Roberts D (2012). Geochemistry of Amphibolite-Facies Volcanics and Gabbros of the Støren Nappe in Extensions West and Southwest of Trondheim, Western Gneiss Region, Norway: A Key to Correlations and Paleotectonic Settings. American Journal of Science 312 (4): 357-416. https://doi.org/10.2475/04.2012.01

Irvine TN, Baragar WRA (1971). A Guide to the Chemical Classification of the Common Volcanic Rocks. Canadian Journal of Earth Science 8: 523-548. https://doi.org/10.1139/e71-055

Janoušek V, Farrow CM, Erban V (2006). Interpretation of whole-rock geochemical data in igneous geochemistry: introducing Geochemical Data Toolkit (GCDkit). Journal of Petrology 47 (6): 1255-1259. https://doi.org/10.1093/petrology/egl013

Ludwig KR (2003) Isoplot 3.00: A geochronological toolkit for Microsoft Excel. Berkeley Geochronology Center, Berkeley, 70.

Michard A (1989). Rare earth element systematics in hydrothermal fluids. Geochimica et Cosmochimica Acta 53 (3): 745-750. https://doi.org/10.1016/0016-7037(89)90017-3

Okay Aİ, Siyako M, Bürkan KA (1990). Biga Yarımadası'nın Jeolojisi ve Tektonik Evrimi. Türkiye Petrol Jeologları Derneği Dergisi, 2 (1): 83-121 (in Turkish).

Okay Aİ, Satır M, Maluski H, Siyako M, Monie P et al. (1996). Paleo- and Neo- tethyan Events in Northwest Turkey. In: Yin A, Harrison M (eds) The Tectonic Evolution of Asia. Cambridge University Press, 420-441.

Okay Aİ, Monié P (1997). Early Mesozoic subduction in the Eastern Mediterranean: Evidence from Triassic eclogite in northwest Turkey. Geology 25 (7): 595-598. https://doi.org/10.1130/0091-7613(1997)025<0595:EMSITE>2.3.CO;2

Okay Aİ, Satır M (2000). Upper Cretaceous Eclogite-Facies Metamorphic Rocks from the Biga Peninsula, Northwest Turkey. Turkish Journal of Earth Sciences, 9 (2-3): 47-56.

Okay Aİ, Göncüoğlu MC (2004). Karakaya Complex: a review of data and concepts. Turkish Journal of Earth Sciences, 13 (2): 77-95

Paton C, Hellstrom J, Paul B, Woodhead J, Hergt J (2011). Iolite: Freeware for the visualisation and processing of mass spectrometric data. Journal of Analytical Atomic Spectrometry 26 (12): 2508-2518. https://doi.org/10.1039/C1JA10172B

Pearce JA, Cann JR (1973). Tectonic setting of basic volcanic rocks determined using trace element analyses. Earth and Planetary Science Letters 19 (2): 290-300. https://doi.org/10.1016/0012-821X(73)90129-5

Pearce JA (1982). Trace Element Characteristics of Lavas from Destructive Plate Boundaries. In: Thorpe, R.S., Ed., Andesites, Wiley, Hoboken, 528-548.

Peate DW (1997). The Parana-Etendeka Province. In: Large Igneous Provinces. Mahoney, J.J. Coffin, M.F. (Editors), American Geophysical Union, Washington D.C. 217-245. https://doi.org/10.1029/GM100p0217

Rollinson HR (1993). Using geochemical data: Evaluation, presentation, interpretation. Longman Scientific and Technical, Wiley, New York, 384. https://doi.org/10.4324/9781315845548

Saner S (1977). Geyve-Osmaneli-Gölpazarı-Taraklı alanının jeolojisi: Eski çökelme ortamları çökelmenin evrimi. PhD, İstanbul Üniversitesi, 312 p. (in Turkish).

Sláma J, Kosler J, Condon DJ, Crowley JL, Gerdes A et al. (2008). Plešovice zircon - A new natural reference material for U-Pb and Hf isotopic microanalysis. Chemical Geology 249 (1-2): 1-35. https://doi.org/10.1016/j.chemgeo.2007.11.005

Şengör AMC, Yılmaz Y (1981). Tethyan evolution of Turkey: A plate tectonic approach. Tectonophysics, 75 (3-4): 181-241. https://doi.org/10.1016/0040-1951(81)90275-4

Şengör AMC, Yılmaz Y, Sungurlu O (1984). Tectonics of the Mediterranean Cimmerides: nature and evolution of the western termination of Paleo-Tethys. In: The geological evolution of the eastern Mediterranean (Ed AH.F. Robertson), Geological Society, London, Special Publication, 17: 77-112. https://doi.org/10.1144/gsl.sp.1984.017.01.04

Tekkaya İ (1973). Gülpınar'daki fosil Bovidae kalıntıları hakkında bir not. Türkiye Jeoloji Bülteni 16 (2): 77-87 (in Turkish).

Tunç İO (2008). Bayramiç (Çanakkale) Güneyindeki Kazdağ Masifi Kayalarının Jeolojisi. Yüksek Lisans Tezi, Çanakkale Onsekiz Mart Üniversitesi, Fen Bilimleri Enstitüsü, p. 112 (in Turkish).

Tunç İO, Yiğitbaş E, Şengün F, Wazeck J, Hofmann M et al. (2012). U-Pb Zircon Geochronology of Northern Metamorphic Massifs in the Biga Peninsula (NW Anatolia-Turkey): New Data and a New Approach to Understand the Tectonostratigraphy of the Region. Geodinamica Acta 25 (3-4): 202-225. https://doi.org/10.1080/09853111.2013.877242

Wiedenbeck M, Hanchar JM, Peck WH, Sylvester P, Valley J et al. (2004). Further characterisation of the 91500 zircon crystal. Geostandards and Geoanalytical Research 28 (1): 9-39. https://doi.org/10.1111/j.1751-908X.2004.tb01041.x

Wilson M (1989). Review of Igneous Petrogenesis: A global Tectonic Approach. Terra Nova 1 (2): 218-222. https://doi.org/10.1111/j.1365-3121.1989.tb00357.x

Wood DA (1980). The application of a Th-Hf-Ta diagram to problems of tectonomagmatic classification and to establishing the nature of crustal contamination of basaltic lavas of the British Tertiary volcanic province. Earth and Planetary Science Letters 50 (1): 11-30. https://doi.org/10.1016/0012-821X(80)90116-8

Yılmaz Y (1977). Bilecik-Söğüt dolayındaki Eski Tümel Karmaşığının petrojenik evrimi. Doçentlik Tezi, İstanbul Üniversitesi Fen Fakültesi, 169 s. (in Turkish).

Yılmaz Y, Tüysüz O, Yiğitbaş E, Genç ŞC, Şengör AMC (1997). Geology and tectonic evolution of the Pontides. A.G. Robinson (Ed.), Regional and Petroleum Geology of the Black Sea and Surrounding Regions, AAPG Memoir 68: 183-226. https://doi.org/10.1306/M68612C11

Yiğitbaş E, Şengün F, Tunç İO (2009a). Biga ve Gelibolu Yarımadaları'nda Yüzeyleyen Mesozoyik Yaşlı Kaya Topluluklarının Jeolojisi ve Stratigrafik Özellikleri. TÜBİTAK ÇAYDAG-108Y232 Nolu Proje Raporu (in Turkish).

Yiğitbaş E, Tunç İO, Şengün F (2009b). Biga Yarımadası'nda Bazı Temel Jeolojik Sorunlar. 62. Türkiye Jeoloji Kurultayı Bildiri Özleri Kitabı, 458-459 (in Turkish).

Yiğitbaş E, Tunç İO, Şengün F (2014a). Kazdağ Masifinin Düşük Dereceli Metamorfik Zarfı; Sakarya Zonunun Tektonik Gelişimi İçindeki Anlam ve Önemi. 67. Türkiye Jeoloji Kurultayı, 542-543 (in Turkish).

Yiğitbaş E, Şengün F, Tunç İO (2014b). Biga Yarımadası'nda (KB Anadolu) Neojen Öncesi Tektonik Birlikler ve Bölgenin Jeodinamik Evrimine Yeni Bir Bakış. TÜBİTAK ÇAYDAG-110Y281 Nolu Proje Raporu (in Turkish).

Yiğitbaş E, Tunç İO, Özkara Ö (2018). Sakarya Zonunun Kuzeybatı Kesimlerinde Alt Karakaya Kompleksi ve Nilüfer Biriminin Yaşı, Stratigrafik ve Yapısal Nitelikleri ve Jeolojik Anlamı. TÜBİTAK ÇAYDAG-115Y214 Nolu Proje Raporu (in Turkish).

Yiğitbaş E, Tunç İO (2020). Biga Yarımadası'nda Sakarya Zonunun Prekambriyen Metamorfk Kayaları; Geç Ediyakaran Gondwanaland Aktif Kıta Kenarı. Türkiye Jeoloji Bülteni 63 (3): 277-302. https://doi.org/10.25288/tjb.589144 (in Turkish).

Appendix

Appendix 1. Table showing the major oxides, trace elements, and rare earth element analysis results of metavolcanic samples.

Major oxides (wt%)	2101	2204	2205	2206	2209
SiO_2	66.9	37.4	48.3	67.5	57.3
TiO_2	0.6	0.94	0.77	0.59	0.55
Al_2O_3	15.25	26.3	17.2	15.45	14.35
Fe_2O_3	4.99	9.29	9.77	4.73	9.59
MnO	0.1	0.09	0.14	0.06	0.15
MgO	2.16	6.83	4.45	1.72	6.48
CaO	0.27	3.73	5.12	0.89	4.54
K_2O	2.82	6.14	1.07	2.39	1.17
Na_2O	3.3	0.1	4.12	5.06	2.77
P_2O_5	0.18	0.25	0.17	0.12	0.1
LOI	3.41	8.81	7.36	2.05	4.35
Sum	99.98	99.88	98.47	100.56	101.35
Trace elements (ppm)	**2101**	**2204**	**2205**	**2206**	**2209**
Ti	3597	5635	4616	3537	3297
Cr	17	33	20	12	286
Rb	63.1	182	31.4	47.1	17.2
Sr	60.7	7.5	140	134	246
Cs	1.22	2.91	1	2.76	0.44
Ba	1590	598	111	345	686
V	76	260	238	72	214
Ta	0.6	0.2	0.3	0.2	0.3
Nb	9.87	13.7	6.93	4.8	5.87
Zr	134	162	78	114	88
Hf	3.68	4.66	2.05	3.15	2.34
Th	6.66	8.35	2.71	4.27	4.19
U	2.31	1.14	0.73	1.28	1.64
Y	20.8	20.5	18.6	27.7	16.6
La	24.3	22.8	17.2	14.3	15
Ce	43.7	47.9	34.3	29.7	26
Pr	4.68	5.51	4.05	3.38	3.16
Nd	16.4	23.8	16.2	15.9	12.2
Sm	3.52	4.97	3.6	3.46	2.28
Eu	0.83	0.78	0.93	1.26	0.82
Gd	3.38	4.88	3.55	4.57	2.88
Tb	0.5	0.68	0.59	0.81	0.46
Dy	3.45	4.23	3.65	4.53	2.9
Ho	0.7	0.91	0.67	1.02	0.67
Er	2.2	2.56	2.19	3.2	1.63
Tm	0.29	0.31	0.24	0.48	0.22
Yb	2.48	2.34	2.01	3.05	1.76
Lu	0.38	0.38	0.31	0.46	0.28
Sn	0.8	1.5	0.7	1.4	0.25
LOI Factor	1.04	1.10	1.08	1.02	1.04

Appendix 2. LA-ICP-MS zircon U-Pb results of diabase sample (2202). (The data are sorted by $^{206}Pb/^{238}U$ ages from youngest to oldest. Shaded data represent the results of the concordant analysis in the range of 90%–110%.)

		Concentrations				Ages				
Spot no.	Th/U	$^{207}Pb/^{235}U$	2σ (abs)	$^{206}Pb/^{238}U$	2σ (abs)	$^{206}Pb/^{238}U$	2σ (abs)	$^{207}Pb/^{235}U$	2σ (abs)	% conc
a81	0.389	0.172704	0.053047	0.023613	0.001754	150.4	10.7	156.0	45.0	96.4
a14	0.371	0.198693	0.049225	0.024475	0.001467	155.8	8.7	172.2	40.9	90.5
a99	0.354	0.165515	0.042405	0.024560	0.001526	156.3	9.1	142.6	35.3	109.6
a6	0.442	0.160933	0.023938	0.025086	0.001091	159.7	6.1	147.3	20.1	108.4
a104	0.464	0.180854	0.053199	0.025148	0.001722	160.0	10.4	157.7	44.2	101.4
a8	0.456	0.192914	0.043058	0.025230	0.001551	160.5	9.2	170.1	36.4	94.3
a19	0.304	0.291502	0.124280	0.025329	0.002467	161.1	15.2	224.9	92.6	71.6
a7	0.457	0.200434	0.048836	0.025334	0.002688	161.2	16.6	181.6	42.1	88.7
a66	0.511	0.183900	0.027674	0.025367	0.001130	161.4	6.4	167.5	23.1	96.4
a79	0.356	0.222603	0.183808	0.025438	0.001581	161.8	9.4	117.9	27.5	137.2
a62	0.389	0.183075	0.022593	0.025493	0.001139	162.2	6.5	167.5	19.1	96.9
a25	0.531	0.356435	0.151518	0.025524	0.002917	162.3	18.0	265.6	110.1	61.1
a30	0.338	0.189545	0.032229	0.025558	0.001093	162.6	6.1	170.1	23.3	95.6
a12	0.628	0.231730	0.104347	0.025636	0.002106	162.9	12.8	145.9	77.9	111.7
a84	0.385	0.183264	0.033277	0.025655	0.001970	163.2	12.0	173.4	30.8	94.1
a34	0.391	0.191667	0.039057	0.025651	0.001262	163.2	7.3	167.9	30.8	97.2
a111	0.436	0.185611	0.095016	0.025649	0.002865	163.2	17.7	164.4	78.1	99.3
a108	0.435	0.216328	0.071856	0.025830	0.002417	164.2	14.9	175.2	58.9	93.7
a20	0.353	0.200279	0.055281	0.025939	0.001827	164.9	11.0	168.8	45.0	97.7
a23	0.450	0.197864	0.050568	0.025712	0.001470	165.1	9.2	171.4	43.5	96.3
a40	0.506	0.183600	0.045867	0.025997	0.002377	165.3	14.6	165.3	38.4	100.0
a91	0.389	0.185055	0.047607	0.026020	0.001651	165.5	9.9	160.3	39.0	103.2
a103	0.000	0.215550	7.094668	0.079760	0.066080	165.8	241.1	734.2	283.1	22.6
a29	0.410	0.169550	0.060117	0.026093	0.003517	165.9	21.8	154.1	51.6	107.7
a68	0.452	0.169981	0.020026	0.026082	0.001284	165.9	7.4	160.7	18.1	103.3
a16	0.438	0.247585	0.062244	0.026093	0.001861	165.9	11.2	209.3	50.3	79.3
a106	0.484	0.232737	0.055118	0.026173	0.001852	166.5	11.2	204.2	45.0	81.5
a46	0.357	0.203383	0.055105	0.026217	0.001753	166.8	10.5	181.9	45.1	91.7
a31	0.487	0.488930	0.151064	0.026239	0.001970	166.9	12.0	357.5	97.2	46.7
a27	0.316	0.185707	0.034177	0.026240	0.001337	166.9	7.8	164.6	28.7	101.4
a65	1.047	0.200072	0.031019	0.026374	0.001451	167.7	8.5	180.6	26.3	92.9
a102	0.535	0.231071	0.099512	0.026388	0.002311	167.8	14.2	190.0	78.9	88.3
a89	0.327	0.204907	0.042244	0.026391	0.002036	167.8	12.4	183.4	34.7	91.5
a64	0.352	0.444042	0.217781	0.026439	0.003408	168.0	21.2	317.9	149.1	52.9
a110	0.372	0.164025	0.027932	0.026585	0.001158	169.1	6.5	149.9	23.7	112.8
a2	0.393	0.377108	0.116119	0.026613	0.002030	169.2	12.3	304.9	88.0	55.5
a67	0.680	0.227591	0.072626	0.026643	0.001714	169.4	10.3	179.1	57.4	94.6
a98	0.454	0.268010	0.107999	0.026949	0.002402	171.1	14.7	180.0	83.3	95.1
a69	0.365	0.221582	0.073833	0.027308	0.001873	173.5	11.3	179.0	55.8	97.0

Appendix 2. Continued

a55	0.474	0.201881	0.132084	0.027402	0.003309	174.2	20.5	180.6	111.9	96.5
a85	0.393	0.209909	0.047345	0.027447	0.002363	174.3	14.4	183.8	38.7	94.9
a101	0.418	0.242893	0.093812	0.027484	0.002581	174.4	15.8	180.1	76.9	96.8
a35	0.360	0.178863	0.058247	0.027543	0.002591	175.1	15.9	163.5	48.7	107.1
a107	0.348	0.261160	0.092772	0.027567	0.002711	175.2	16.7	217.4	74.1	80.6
a33	0.792	0.180337	0.067527	0.027732	0.002120	176.3	12.9	162.5	58.5	108.5
a39	0.362	0.210930	0.048262	0.027879	0.001569	177.1	9.2	181.0	34.5	97.8
a92	0.462	0.177507	0.041293	0.027958	0.002392	177.5	14.5	155.4	33.1	114.2
a28	0.295	0.228688	0.051246	0.028053	0.002117	178.2	12.8	198.7	40.7	89.7
a36	0.398	0.215445	0.059851	0.028147	0.001992	178.9	12.0	206.0	58.8	86.8
a37	0.413	0.212689	0.058230	0.028163	0.002136	178.9	12.9	185.4	48.4	96.5
a15	0.518	0.658295	0.279242	0.028642	0.005081	181.6	31.5	438.4	155.6	41.4
a52	0.399	0.658105	0.168182	0.029422	0.003223	186.6	19.8	460.8	99.3	40.5
a54	0.338	0.701326	0.705401	0.031395	0.005162	198.1	30.6	158.7	65.7	124.8
a22	0.412	0.310439	0.350870	0.031422	0.006331	198.9	39.5	133.0	257.1	149.6
a38	0.330	0.701374	0.407835	0.031642	0.006505	199.9	40.1	314.8	271.4	63.5
a96	0.523	1.501540	0.633873	0.035614	0.004985	224.2	29.8	622.6	147.1	36.0
a82	0.000	1.791959	5.771679	0.096080	0.081038	292.0	422.3	2391.7	446.4	12.2
a57	0.228	0.590486	0.120775	0.051038	0.003040	320.4	17.6	475.3	71.3	67.4
a41	0.000	0.163694	5.332470	0.065650	0.056103	340.3	333.3	2512.6	398.4	13.5
a77	0.796	0.970201	0.164465	0.091068	0.004048	561.1	21.5	690.6	54.0	81.3